

Analysis of the Isothermal Structure Development in Waxy Crude Oils under Quiescent Conditions

J. A. Lopes-da-Silva*[†] and João A. P. Coutinho[‡]

QOPNA Unit and CICECO, Department of Chemistry, University of Aveiro, 3810-193 Aveiro, Portugal

Received June 24, 2007. Revised Manuscript Received August 29, 2007

Isothermal crystallization and structure development was studied for three different waxy crude oils. The transformation from sol to gel was followed by small-amplitude dynamic rheometry, which closely tracks the development of the three-dimensional network as the initially formed crystallites grow, aggregate, and interact with each other. The kinetics of the crystallization-induced gelation was analyzed with the phenomenological Avrami model. The analysis was performed for a temperature range of about 15 K and was limited to the early stages of transformation. Both the Avrami exponent n and the rate constant k are dependent on the crystallization temperature, meaning that the nucleation and crystal growth mechanisms and rates are dependent on the degree of supercooling. Higher Avrami constants and lower Avrami coefficients (higher rate of crystal growth) were observed under higher supercooling conditions. The results discussed allowed the predominant mechanisms for nucleation and crystal growth, occurring as a function of temperature (i.e., supercooling degree) and waxy crude oil composition, to be defined.

Introduction

The development of solid deposits in crude oils is a well-known and recurrent problem for the oil industry. This problem is caused by the crystallization of paraffins in surfaces kept at temperatures below the cloud point of the oil. The formation of the solid phase is mainly related to the presence of waxes, which are essentially a multicomponent mixture of high molecular weight saturated hydrocarbons, predominantly paraffins, in the range C18–C65.¹ The deposits thus formed have a gel-like structure, formed by a three-dimensional (3D) network of interlocking paraffin crystals that creates a highly porous yet rigid structure full of entrapped oil.^{2,3}

Paraffin's crystallization occurs by the classical nucleation and growth mechanisms.^{4,5} Nucleation and growth events under adequate thermodynamic conditions (i.e., supercooling and supersaturation) lead to the formation of submicrometer primary crystallites from the complex hydrocarbon mixture. These crystallites associate into micrometer-range particles, which further aggregate into larger structures (i.e., clusters), and finally, they form structures which prevail the entire mass of the material. The continuous 3D paraffin network, which traps the liquid component, is stabilized essentially by van der Waals forces.

The characteristics of these physical gels are known to undergo a change with time, becoming harder, richer in heavier

paraffins, and with lower amounts of entrapped oil.^{6–8} The mechanism of aging has been explained by a diffusion transport within the porous structure of the gel driven by temperature–composition gradients⁹ and also by Ostwald ripening specially in the absence of temperature–composition gradients.¹⁰

Rheological techniques have been used and their reliability has been demonstrated to study crystallization kinetics in diverse systems such as polymer crystallization,^{11–15} growth kinetics of fibrillar networks of molecular organogels,^{16,17} fat crystal gelation,¹⁸ and starch retrogradation.¹⁹ In many cases the evolution of the storage modulus, obtained from dynamic mechanical methods, allowed the crystallization kinetics to be evaluated and also the nucleation and growth characteristics to be determined.^{18,20,21} Several of these studies have also applied the Avrami framework to characterize the crystallization and

* Corresponding author. E-mail: jsilva@dq.ua.pt. Telephone: +351-234370360. Fax: +351-234370084.

[†] QOPNA Unit.

[‡] CICECO.

(1) Srivastava, S. P.; Handoo, J.; Agrawal, K. M.; Joshi, G. C. *J. Phys. Chem. Solids* **1993**, *54*, 639–670.

(2) Dirand, M.; Chevallerier, V.; Provost, E.; Bouroukba, M.; Petitjean, D. *Fuel* **1998**, *77*, 1253–1260.

(3) Singh, P.; Fogler, H. S.; Nagarajan, N. *J. Rheol.* **1999**, *43*, 1437–1459.

(4) Dirand, M.; Bouroukba, M.; Chevallerier, V.; Petitjean, D.; Behar, E.; Ruffier-Meray, V. *J. Chem. Eng. Data* **2002**, *47*, 115–143.

(5) Paso, K.; Senra, M.; Yi, Y.; Sastry, A. M.; Fogler, H. S. *Ind. Eng. Chem. Res.* **2005**, *44*, 7242–7254.

(6) Creek, J. L.; Lund, H. J.; Brill, J. P.; Volk, M. *Fluid Phase Equilib.* **1999**, *158–160*, 801–811.

(7) Cordoba, A. J.; Schall, C. A. *Fuel* **2001**, *80*, 1279–1284.

(8) Wu, C. H.; Wang, K. S.; Shuler, P. J.; Tang, Y.; Creek, J. L.; Carlson, R. M.; Cheung, S. *AIChE J.* **2002**, *48*, 2107–2110.

(9) Singh, P.; Venkatesan, R.; Fogler, H. S.; Nagarajan, N. *AIChE J.* **2000**, *46*, 1059–1074.

(10) Coutinho, J. A. P.; Lopes da Silva, J. A.; Ferreira, A.; Soares, M. R.; Daridon, J. L. *Petrol. Sci. Technol.* **2003**, *21*, 381–391.

(11) Khanna, Y. P. *Macromolecules* **1993**, *26*, 3639–3643.

(12) Boutahar, K.; Carrot, C.; Guillet, J. *Macromolecules* **1998**, *31*, 1921–1929.

(13) Alig, I.; Tadjbakhsh, S.; Floudas, G.; Tsitsilianis, C. *Macromolecules* **1998**, *31*, 6917–6925.

(14) Kelarakis, A.; Mai, S. M.; Booth, C.; Ryan, A. J. *Polymer* **2005**, *46*, 2739–2747.

(15) Acierno, S.; Di Maio, E.; Iannace, S.; Grizzuti, N. *Rheol. Acta* **2006**, *45*, 387–392.

(16) Liu, X. Y.; Sawant, P. D. *Adv. Mater.* **2002**, *14*, 421–426.

(17) Huang, X.; Terech, P.; Raghavan, S. R.; Weiss, R. G. *J. Am. Chem. Soc.* **2005**, *127*, 4336–4344.

(18) Toro-Vazquez, J. F.; Rangel-Vargas, E.; Dibildox-Alvarado, E.; Charó-Alonso, M. A. *Eur. J. Lipid Sci. Technol.* **2005**, *107*, 641–655.

(19) Mita, T. *Carbohydr. Polym.* **1992**, *17*, 269–276.

(20) Gauthier, C.; Chailan, J. F.; Chauchard, J. *Makromol. Chem.* **1992**, *193*, 1001–1009.

(21) Teh, J. W.; Blom, H. P.; Rudin, A. *Polymer* **1994**, *35*, 1680–1687.

structure development kinetics. Nevertheless, to ascertain relationships between the transformed fraction and the rheological behavior during crystallization is not a simple task and still remains a topic open to discussion.¹² The sensitivity of the viscoelastic measurements to follow the nucleation and growth processes appears to change for different semicrystalline polymers. For several polyolefins and triacylglycerides, the parameters obtained through oscillatory rheometry closely followed the crystallization progress, particularly at the stages of the onset of nucleation and crystal growth, and the rheological changes were observed at very low crystallinity,^{22–24} whereas other reports showed rheological properties changing only when a relatively high degree of crystallinity was reached.¹⁵

The degree of crystallinity (estimated by the Avrami equation) at the gel point, although dependent on the crystallization temperature, is typically very low.^{25,26} In the case of paraffin crystallization, it is also commonly observed that a low amount of solids are needed to form a gel.^{3,27} In addition, rheological measurements on waxy crude oil gels have shown that the rheological approach is very sensitive to a very low amount of solids.²⁸ This behavior suggests that only a few junctions are necessary to form a sample spanning network.

Investigation of the kinetics of wax crystallization is significant both from the theoretical and practical point of view. Of theoretical importance is the mechanism of formation of these colloidal-type gels and the knowledge on the structural organization of the interacting crystallite entities. The practical importance arises from the influence of crystallization-induced gelation in waxy crude oils on the framework of crude oil production and transportation.

In the work presented here, the isothermal crystallization-induced gelation of waxy crude oils under quiescent conditions is reported. The approach followed was based on the temporal changes in the storage modulus to follow the kinetics of gelation, obtained from rheological measurements performed under oscillatory shear at very small strains, at different curing temperatures. The rheological response was interpreted as a consequence of structure development generated by the crystalline morphology, the crystallite cluster formation, and the interaction between these entities throughout the remaining liquid phase. The kinetic behavior was analyzed using the Avrami model.²⁹

Experimental Section

Materials. Three crude oils obtained directly from oil companies, with different origins and wax compositions, were used in this study. Their main characteristics are shown in Table 1. The asphaltene content in all the crudes is negligible.

Sample Characterization. The cloud point of the crude oils, or the temperature (WAT), was measured by cross-polarized microscopy. Pour points were determined according to the ASTM method

Table 1. Properties of the Crude Oils^a

sample	oil type ^b	wax content ^c (wt %)	wax content ^d (wt %)	M_w	PP (°C)	WAT (°C)
A	gas condensate	6.8	6.8	176	15	45
B	paraffinic oil	33	23	216	35	57
C	heavy paraffinic oil	35	21	286	40	73

^a M_w , oil average molecular weight; PP, pour point (ASTM D5853); WAT, temperature (CPM). ^b According to oil supplier. ^c Total wax (acetone precipitation). ^d Saturates (after removal of polar material).

(D-5853). The total wax content was measured by following a modified UOP standard method 46 as proposed by Musser and Kilpatrick.³⁰ The waxes are precipitated by a mixture of acetone and petroleum ether (3:1 v/v), cooled at -20 °C, and then filtered. The solid obtained is the total wax content. The saturated waxes are separated from the aromatics and polar material by chromatography on a 50 cm silica gel column with *n*-heptane. Both oil B and oil C present about 1/3 of precipitated solids other than saturated waxes.

Rheological Measurements. The oscillatory shear experiments were performed using a controlled stress rheometer (AR1000, TA Instruments) fitted with a parallel plate measuring system (4 cm diameter, roughened surface, 1 mm gap). The temperature was controlled to within 0.1 °C by a Peltier plate. Each sample was initially heated to a temperature 15 K above its cloud point (WAT), for 1 h, to erase any previous thermal history or any possible waxy structure. The sample was loaded into the rheometer plate, preset at the same temperature, and covered with a solvent trap to minimize evaporation. Two different experiments were performed: (i) isochronal temperature scans at oscillatory frequency (ω) 1 rad/s with a heating/cooling rate of 0.2 °C/min, (ii) isochronal/ isothermal time scans at ω 1 rad/s and for different temperatures below the WAT. For the isothermal time sweep tests, the sample was quickly quenched (6 °C/min) “in situ”, from the pretreatment temperature to the desired temperature of curing. The oscillation amplitude was controlled to obtain a 0.05% maximum strain in the sample, in order to avoid a perturbation of the crystallization-induced gelation caused by the measuring solicitation. It has been previously shown that similar systems are quite sensitive to the applied strain and that this value is within the linear viscoelastic regime.²⁸ The use of small strains ensures that the rheological parameters are only time and temperature dependent avoiding the crystallization kinetics to be modified by shearing.

Isothermal Kinetic Analysis. The isothermal crystallization kinetics of the crude oil samples was studied on the basis of the rheological data and on the Avrami model with induction time (see Supporting Information for further details):

$$X(t) = 1 - e^{-[k(t - t_0)]^n} \quad (1)$$

where $X(t)$ is the relative crystallinity at time t , k and n are constants with respect to time, and t_0 denotes for the induction time (defined as the time delay to observe the beginning of these variations). We decide on the analysis of k in this form because then it is not dependent on n and its dimensions are given in $(\text{time})^{-1}$.

According to the rheological approach followed in this study, the reaction advance was assumed to be linearly related to the increase in storage modulus (G') during curing of the waxy crude oil. Therefore, the fractional extent of crystallization ($X(t)$) can be approximated by

$$X(t) = (G'_t - G'_0)/(G'_\infty - G'_0) \quad (2)$$

where G'_t is the storage modulus at time t , G'_0 is the initial modulus value (at t_0), and G'_∞ is the pseudo-equilibrium storage modulus. A similar approach has been used to describe the crystallization kinetics of different semicrystalline systems.^{11,12,20,31,32}

(30) Musser, B. J.; Kilpatrick, P. K. *Energy Fuel* **1998**, *12*, 715–725.

(31) Sherman, P. *Industrial Rheology*; Academic Press: London, U.K., 1979; pp 188–190.

(22) Pogodina, N. V.; Winter, H. H. *Macromolecules* **1998**, *31*, 8164–8172.

(23) Horst, R. H.; Winter, H. H. *Macromolecules* **2000**, *33*, 130–136.

(24) Gelfer, M.; Horst, R. H.; Winter, H. H.; Heitz, A. M.; Hsu, S. L. *Polymer* **2003**, *44*, 2363–2371.

(25) Kim, C. Y.; Kim, Y. C.; Kim, S. C. *Polym. Eng. Sci.* **1993**, *33*, 1445–1451.

(26) Schwittay, C.; Mours, M.; Winter, H. H. *Faraday Discuss.* **1993**, *101*, 93–104.

(27) Coutinho, J. A. P.; Mirante, F.; Ribeiro, J. C.; Sansot, J. M.; Daridon, J. L. *Fuel* **2002**, *81*, 963–967.

(28) Lopes da Silva, J. A.; Coutinho, J. A. P. *Rheol. Acta* **2004**, *45*, 433–441.

(29) (a) Avrami, M. *J. Chem. Phys.* **1939**, *7*, 1103–1112. (b) Avrami, M. *J. Chem. Phys.* **1940**, *8*, 212–224. (c) Avrami, M. *J. Chem. Phys.* **1941**, *9*, 177–184.

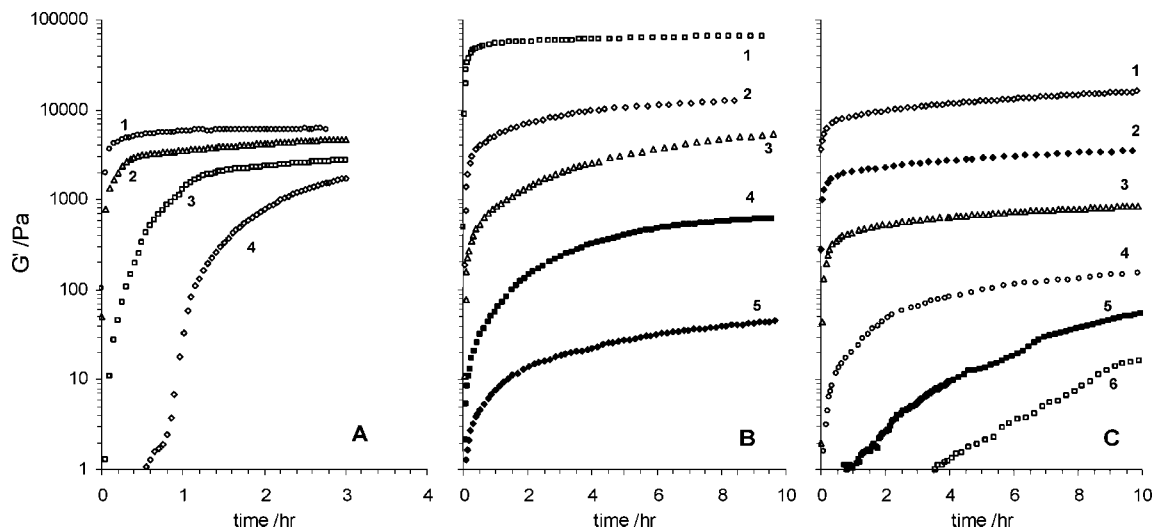


Figure 1. Representative cure curves showing the time dependence of the storage modulus (G') during isothermal crystallization for different quenching temperatures: (A) Oil A: 1, 18 °C; 2, 20 °C; 3, 24 °C; and 4, 26 °C. (B) Oil B: 1, 32 °C; 2, 36 °C; 3, 38 °C; 4, 40 °C; and 5, 42 °C. (C) Oil C: 1, 35 °C; 2, 40 °C; 3, 45 °C; 4, 48 °C; 5, 50 °C; and 6, 52 °C.

The temperature dependence of the crystallization rate was analyzed by the Arrhenius equation:

$$k = A \exp(-E_a/RT) \quad (3)$$

where A is the Arrhenius pre-exponential factor, E_a is the activation energy, R is the gas constant, T is the absolute temperature, and k is the rate constant obtained from the Avrami equation.

Results and Discussion

Isothermal Structure Development. Isochronal cooling tests (0.2 °C/min, 1 rad/s) were performed as preliminary measurements to define the isothermal crystallization temperatures most suitable for each sample (see Figure S1, Supporting Information). A sharp increase in the viscoelastic moduli was observed when the temperature reached a certain value, characteristic of each oil sample, below the cloud point (WAT) but well above the pour point. This characteristic temperature associated to the sol–gel transition was defined as the point at which G' (elastic response) became greater than G'' (viscous response).²⁸ According to this criterion, the observed gelation temperatures were 33.0 °C, 41.6 °C, and 50.5 °C, for oil samples A, B, and C, respectively.

The isothermal annealing of the oils was performed for different temperatures, as of close to the gelation temperature, that is, at about 20 K lower than the WAT of each sample and within a range of about 10–15 K.

The dynamic rheological parameters (G' , G'' , $\tan \delta$) were very sensitive to the structure change going along with the crystallization process. Representative isothermal cure curves, showing the time dependence of the storage modulus (isothermal runs) recorded after temperature jumps from an initial temperature above the WAT to different crystallization temperatures, are shown in Figure 1. One can observe that the crystallization kinetics is substantially affected by the crystallization temperature.

The storage modulus increases as a result of the increase of volume fraction of the solid crystalline phase, crystal growth, and increasing junction zones density between wax crystals. Under higher degrees of supercooling, a rapid increase in the viscoelastic modulus was observed with a great variation during the initial aging period, covering about three orders of magni-

tude. The samples are crystallized rapidly, and the process is characterized by the absence of the induction time. Under lower supercooling conditions, that is, at higher temperatures, close to the gelation temperature, an induction period is perceptible, especially for oils A and C, the aging process is much slower, and the changes in the storage modulus follow an S-shape behavior.

After the rapid increase in elasticity within the gel, G' keeps increasing slightly and continuously as a result of the reinforcement of the network by slower formation and rearrangement of elastic active bonds/junction zones, reaching a pseudo plateau region. A true equilibrium modulus was not reached even after long aging periods, especially for the lower supercooling temperatures, that is, for the lower concentration of crystallized material (after more than 96 h in some cases), meaning a continuous reorganization of the particulate network. This structural re-order and continuous increase of G' with time may be associated to crystal reorganizing to a more perfect state, secondary crystallization, and slow rearrangements within the crystal network.

The corresponding loss moduli (G'') data are omitted for clarity. The sample was initially heated 15 K above its WAT and rapidly quenched to different final temperatures. The frequency was 1 rad/s, and the strain amplitude was 0.05%.

Avrami Analysis. The data obtained from the isothermal curing were converted into the fractional extent of crystallization ($X(t)$) accordingly to eq 2 (see Figure S2, Supporting Information, for some examples). The kinetic information via the Avrami equation (eq 1) was obtained from the relative degree of transformation ($X(t)$). Examples of the Avrami plots are shown in Figure 2.

The Avrami equation is typically limited to low degrees of crystallinity.³³ At high transformation extent some well-known limitations to the Avrami model, namely, impingement of crystals with one another and occurrence of secondary crystallization, will have an important role. Also, some restrictions to the rheological approach are expected to occur at high curing times related to the lost sensitivity of G' to the growth of crystals/clusters at long-time range. In view of that, we have studied essentially the kinetics of crystallization at its early

(32) Coppola, S.; Acerno, S.; Grizzuti, N.; Vlassopoulos, D. *Macromolecules* **2006**, *39*, 1507–1514.

(33) Sperling, L. H. *Introduction to Physical Polymer Science*, 2nd ed.; John Wiley & Sons: New York, 1992; pp 234–238.

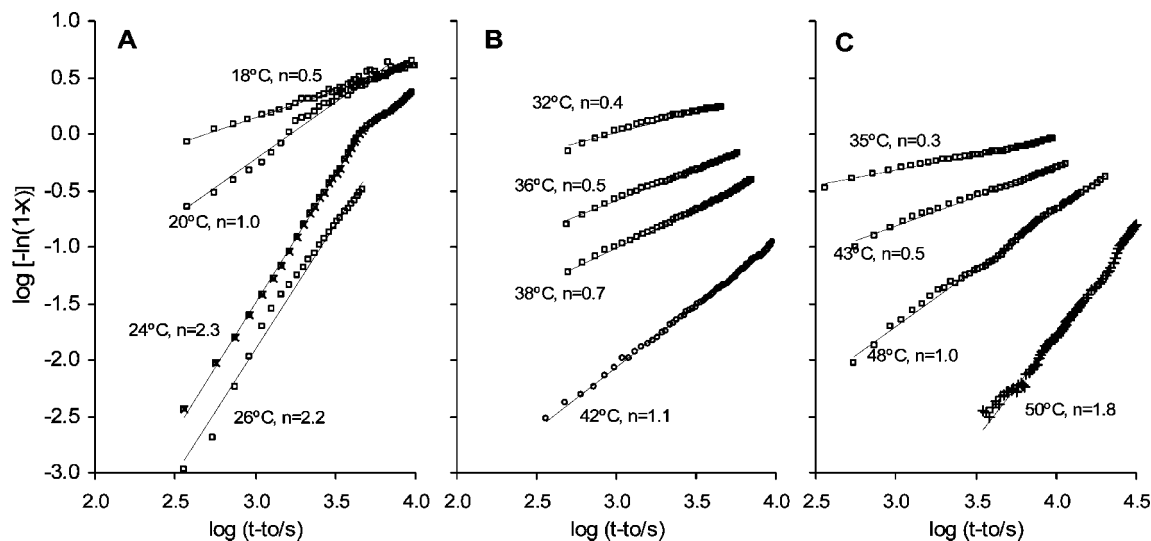


Figure 2. Avrami plots for oils A, B, and C, respectively (according to eqs 1 and 2). Also shown are the Avrami exponents obtained for selected curing temperatures. To illustrate the comparison among oil samples on the basis of equivalent supercooling degree, one may consider oil A at 20 °C, oil B at 32 °C, and oil C at 48 °C, which correspond to a supercooling degree of $\Delta T \approx 25$ °C.

stages and only the initial portion of the crystallization/gelation isotherms was used for determination of the Avrami kinetic constants. Therefore, each curve in Figure 2 corresponds to the initial linear portion obtained for relatively low fractional extent of crystallization. Deviations from linearity were observed at the later stage of crystallization (see, for example, the Avrami plot at 24 °C obtained for oil A). This kind of behavior has been observed for several crystallizable systems and was attributed in many cases to secondary crystallization.^{34–36}

The values of the kinetic parameters determined from the initial linear portion of the Avrami plots are listed in Table S1, Supporting Information.

Both the Avrami exponent n and the rate constant k are dependent on the crystallization temperature (T_c). Consequently, the nucleation and crystal growth mechanisms and rates are expected to be affected by T_c and the degree of supercooling. However, the magnitude of this effect depends on the type of waxy crude oil analyzed, thus pointed out for the important role of the complex oil composition.

The Avrami exponent, n , reflects the nucleation mechanism and growth dimension of the crystals. Figure 3 shows the Avrami exponent values obtained for oils A, B, and C, at different crystallization/gelation temperatures. The different n values as T_c changes mean that a different nucleation and/or crystal growth would take place at different temperatures, thus suggesting the existence of different crystallization mechanisms depending on the degree of supercooling. Generally, the value of n decreases as the crystallization temperature decreases (higher supercooling), indicating that the nucleation events tend to be more instantaneous (compared to sporadic nucleation at higher n values) and the dimensionality of growth of the crystalline material tends to be lower.

The temperature-dependent supersaturation is the driving force of nucleation. For the same oil, at a lower supersaturation (higher temperature), the amount of crystallized material will be much lower and the available free space will be larger. In

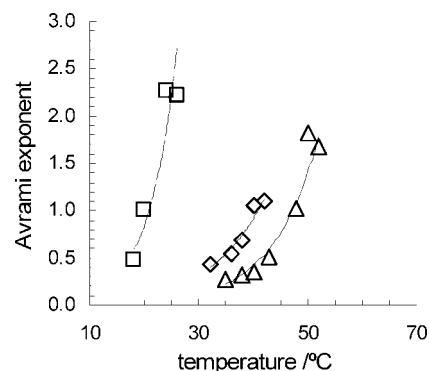


Figure 3. Plot of the Avrami exponent (n) as a function of crystallization temperature, for oils A (\square), B (\diamond), and C (\triangle).

fact, one could expect that both the nucleation mechanism and the crystal morphology will depend strongly on the supersaturation.

Oil A exhibits a remarkable change of Avrami exponent from $n \approx 0.5$ to $n \approx 2$ within a narrow crystallization temperature (from 18 °C to 24 °C). At higher supersaturation/supercooling (lower temperature) instantaneous nucleation is the predominant nucleation mechanism. In addition, the low and fractional n value also indicates that at lower T_c diffusion controlled growth is playing an important role.

At higher T_c (lower supercooling), sporadic nucleation may have a more important role and the Avrami exponents around 2 may be indicative of a two-dimensional growth (disk/platelet) mechanism, in accordance with several reports that described the paraffin crystals as lamellar structures under quiescent conditions.^{37,38}

The Avrami exponents obtained for oils B and C showed a lower dependence on temperature as compared with oil A. Nevertheless, the temperature dependence of the Avrami exponents followed, qualitatively, a similar profile. Especially at lower temperatures the Avrami exponent reaches values inferior to 1.0.

The fractional values obtained in the determination of n might be associated with secondary crystallization occurring during

(34) Wunderlich, B. *Macromolecular Physics*; Academic Press: New York, 1976.

(35) Hwang, J. C.; Chen, C.-C.; Chen, H.-L.; Yang, W. C. O. *Polymer* **2001**, *38*, 4097–4101.

(36) Xiao, J.; Zhang, H.; Wan, X.-H.; Zhang, D.; Zhou, Q.-F.; Woo, E. M.; Turner, S. R. *Polymer* **2002**, *43*, 7377–7387.

(37) Hollander, F. F. A.; Stasse, O.; van Suchtelen, J.; van Enkevort, W. J. P. *J. Cryst. Growth* **2001**, *233*, 868–880.

(38) Kané, M.; Djabourov, M.; Volle, J.-L.; Lechaire, J.-P.; Frebourg, G. *Fuel* **2003**, *82*, 127–135.

crystal growth and/or to the simultaneous development of at least two types of crystals. Confinement at low crystallization temperatures and the presence of high concentrations of non-crystallizable impurities have also been suggested to originate half-order values of n , including Avrami exponents around 0.5, associated to diffusion-controlled crystallization.^{33,39,40} Besides the clear prevalence of diffusion-controlled rate mechanisms, the relatively low n values also point towards heterogeneous (simultaneous) nucleation, which can be explained as due to the complex composition and the probable occurrence of microscopic insoluble particles dispersed randomly in the sol phase, such as impurities that can act as nucleation centers.

Under the temperature range analyzed, the Avrami exponents for oil B did not reach values higher than around 1, but for oil C, under low supercooling, n also reached values close to 2. Given the qualitatively similar behavior of the three oils it would be expected that oil B would present higher Avrami exponents for higher temperatures.

At low supercooling (high temperatures), that is, slow crystallization, the higher Avrami exponents around 2 indicate a nearly bidimensional growth of the individual crystals, essentially as disks or platelets, spanning different domains, with heterogeneous nucleation, while at higher supercooling (lower temperatures), that is, faster crystallization, the crystal growth geometry would be essentially one-dimensional, that is, like rods or needles. These results are in good agreement with visual observations for paraffin crystals formed in hydrocarbon mixtures.

Crude oils are chemically very complex, and the crystallization process in crude oils is necessarily a complex process influenced by many intrinsic and extrinsic factors.

Available literature on the microstructure and morphology of waxy crude crystallite gels agree on one point: the crystallization of paraffins leads to the formation of gels with a very complex morphology, the wax crystals having typical highly nonlinear and irregular characteristics.^{2,41} Moreover, there is a lack of general agreement either on the shape or on the average size of the crystals that form in real waxy crude oils.

Some of the observed discrepancies regarding the crystallite morphology and interactions have been attributed to sample preparation, thermal and shear histories, and methods of analysis. However, it is likely most dependent on the composition complexity of the waxy crude oil. In fact, the kinetic behavior reported at the present work, namely, the strong time and temperature dependence of the crystal growth overlap and interlock processes, supports the complex structural organization of the wax crystal gels as an intrinsic characteristic of these systems.

Temperature Dependence of the Transformation Rate.

The transformation half-time, $t_{1/2}$, is defined as the time at which the extent of crystallization reaches 50% of its final extent. This characteristic time is then proportional to the inverse of the growth rate; the greater the value of $t_{1/2}$, the lower is the rate of the crystallization. The half-times ($t_{1/2}$) calculated from the $X(t)$ versus time curves as a function of the crystallization temperature are shown in Figure 4. Essentially linear relationships between $\log(t_{1/2})$ and T_c were observed for the three crude oils, and the slopes are indicated in the figure. The crystallization half-time ($t_{1/2}$) for all samples increases with the crystallization temperature; that is, the rate of transformation decreases. The lower the temperature (higher degree of supersaturation), the

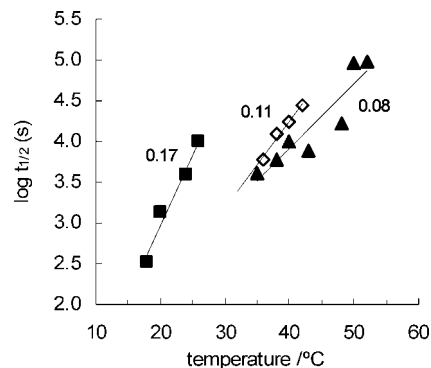


Figure 4. Half-times ($t_{1/2}$) for the isothermal crystallization induced-gelation process as a function of the crystallization temperature, for oils A (■), B (◇), and C (▲). Lines are guides to the eyes, and the inserted numbers are the corresponding slopes.

greater the concentration driving force for crystallization, the smaller and more numerous would be the crystals, and the faster and more probable is gelation. The half-times $t_{1/2}$ for the oils seem to increase with their molecular weight indicating that at similar supercooling degree the paraffinic crystals from heavier oils have more difficulty in growing possibly because of their larger size and the presence of heavy molecules that interfere in the crystal growth. As shown, the dependence on temperature of the half-time values tends to decrease with the oil molecular weight following the order oil A > oil B > oil C.

As expected, the kinetic Avrami rate constant, k , tends to decrease with increasing crystallization temperature. The temperature dependence of k was analyzed using an Arrhenius-type equation (Eq. 3). The overlap of primary nucleation and crystal growth is expected to complicate the interpretation of the temperature dependence of the Avrami rate constant, namely via the habitual Arrhenius model, since the activation energies of the two processes, nucleation and growth, may have different temperature dependencies. Anyway, within the temperature range analysed, the Arrhenius equation seems to describe the data satisfactorily and enables to obtain an estimate of the gelation/crystallization activation energy for this system under isothermal conditions.

Figure 5 shows the Arrhenius plots obtained for oils A, B, and C. The activation energy values were 232 kJ/mol, 236 kJ/mol, and 89 kJ/mol for samples A, B, and C, respectively. Arrhenius-type plots of k values using the reduced temperature, $WAT - T_c$, were also constructed. Despite some scatter in the data, their approximate slopes suggest "activation energies", approximately 1.3 kJ/mol for oil sample A and approximately 0.7 kJ/mol for oils B and C. Insofar as this treatment is meaningful, it suggests that, for the crude oils with higher molecular weight and a more complex composition of the heavy fraction, the aggregation processes and the crystallization-induced gelation are slower.

This is likely explained as due to the presence of paraffins with higher molecular weight that precludes rapid rearrangements and fast coarsening of the crystallites, originating from a slower aging growth of more imperfect crystals that retard crystallization. The presence of heavy compounds that interfere with the crystal growth also contributes to the slower gelation observed and the small dimensions of the paraffin crystals observed in crudes³⁸ when compared with synthetic waxes. This lower transformation rate also supports a predominant role of diffusional mechanisms. In contrast, for the lower molecular weight oil, the higher mobility of the paraffin chains and the

(39) Keith, H. D.; Padden, F. J. *J. Appl. Phys.* **1964**, *35*, 1270–1285.

(40) Xu, J. T.; Fairclough, J. P. F.; Mai, S. M.; Ryan, A. J. *Macromolecules* **2002**, *35*, 6937–6945.

(41) Gao, P.; Zhang, J. J.; Ma, G. X. *J. Phys.: Condens. Matter* **2006**, *18*, 11487–11506.

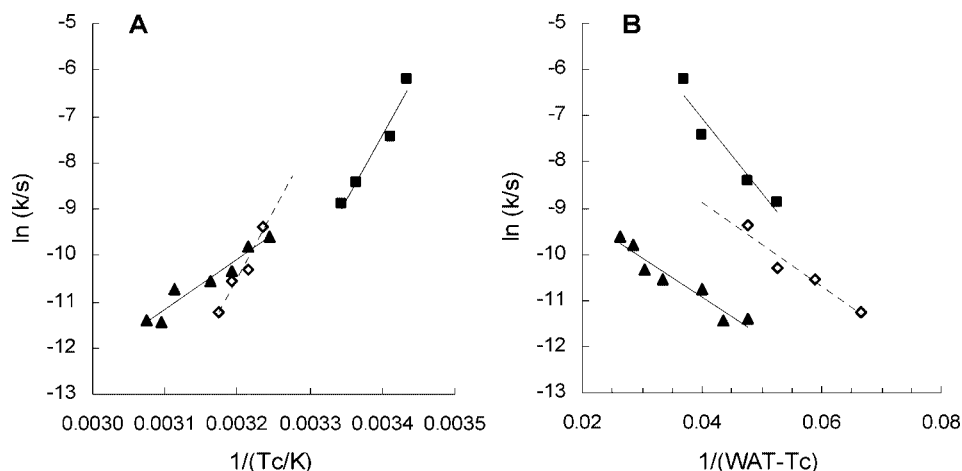


Figure 5. (A) Arrhenius plots for oils A (■), B (◇), and C (▲). The apparent activation energies, calculated from the slope of the linear relationships, are -232 , -236 , and -89 kJ/mol, respectively (accordingly to eq 3). (B) Arrhenius-type plots, considering the Avrami rate constant as a function of the supercooling degree ($WAT - T_c$), for the same samples. The apparent activation energies, calculated from the slope of the linear relationships, are 1.3 , 0.75 , and 0.70 kJ/mol, respectively.

lower amount of other compounds that interfere with the crystal growth cause a higher transformation rate.

Conclusions

Rheological changes have been used to follow the kinetics of crystallization and gelation of three waxy crude oils. The results have been analyzed primarily using an Avrami model. This approach is mainly related to aggregation and self-assembly processes and analyzes the gelation process at a different length scale when compared with other techniques that have been in wider use, for example, differential scanning calorimetry, X-ray, and microscopy.

The crude oils composition is very complex and heterogeneous. The analysis and interpretation of the gelation process is necessarily intricate because of the complex nature of the molecular species that make up the crude oil. Regardless these difficulties, a successful kinetic description of the formation of the space-filling particle network was achieved.

Both the Avrami exponent n and the rate constant k are dependent on the crystallization temperature (T_c), meaning that the nucleation and crystal growth mechanisms and rates are dependent on the degree of supercooling.

The rates of the crystallization-induced gelation decrease with increasing temperature and by increasing the oil complexity composition and molecular weight.

The general changes observed on the Avrami exponent as a function of temperature and oil type point toward a clear predominance of heterogeneous nucleation and diffusion con-

trolled growth, especially at higher supercooling and/or at higher oil complexity composition and molecular weight. The dimensionality of growth of the crystalline material also tends to change from bidimensional under low supercooling conditions to one-dimensional at a higher supercooling extent.

The original Avrami's derivation assumes that a single mode of nucleation is involved, which may not be true because of the complex composition of the samples. Therefore, the possibility of mixed nucleation and growth modes can not be discarded, which makes extracting a direct conclusion from the Avrami's exponents obtained difficult.

Nevertheless, the results obtained enable the predominant nucleation and growth characteristics of the wax crystallites to be defined as related to the gelation kinetics.

Supporting Information Available: Fundamental considerations about the rheological approach and the Kolmogorov–Johnson–Mehl–Avrami model, Avrami kinetic parameters for the different oil samples, a plot of the isochronal cooling runs performed to assess the rheological response of crystallization and structure development as a function of temperature, and plots of the time dependence of the relative degree of transformation ($X(t)$) for the crude oils under isothermal conditions. This material is available free of charge via the Internet at <http://pubs.acs.org>.

Acknowledgment. The authors gratefully acknowledge the financial support from QOPNA and CICECO research units.

EF700357V